

Mechanical properties of Al-Zn-Mg alloys investigated by microhardness measurements

A. JUHÁSZ, P. TASNÁDI, I. KOVÁCS, T. UNGÁR

Institute for General Physics, Eötvös University, Budapest, Hungary

One of the most simple and economic methods of testing the mechanical properties of alloys is the microhardness measurement. In the present paper we report on the results and the interpretation of experiments carried out on a series of Al-Zn-Mg alloys prepared from high purity base materials. The following results were obtained: (a) the incremental microhardness, ΔHV , was related to the microhardness, HV , of high purity Al and can be given as $\Delta HV = 264 (C_{Mg} - 0.25 C_{Zn})$ where C_{Mg} and C_{Zn} are the concentrations of Mg and Zn respectively, in the as-quenched state after solution heat-treatment, (b) the ultimate tensile strength and the microhardness were correlated by the approximation: $HV \cong 3\sigma_U$. ΔHV was investigated in the light of the average radius and the volume fraction of zones forming at room temperature. On the basis of the micro-mechanism of plastic deformation further evidence was found to show that the shearing mechanism is responsible for strengthening by GP zones in Al-Zn-Mg alloys.

1. Introduction

The Al base Al-Zn-Mg alloy system has been widely investigated from both practical as well as fundamental aspects due to their excellent mechanical properties and to the large variety of different types of solid state reactions which can be realised under various conditions [1-5]. Recently, microhardness measurements were used to determine empirical relationships between hardness and tensile parameters for two types of alloy [6].

The correlation between the increment of the yield stress and the microscopic parameters of second phase particles has also been investigated [7] and it was found that the GP zones formed at low temperatures are sheared by the moving dislocations upon deformation. This mechanism of strengthening was observed to operate as long as an average particle radius of about 3 nm is not exceeded. The same investigations have shown that in the case of larger particles (in the present alloy system these are η' and/or η phase particles) the Orowan mechanism is effective in obstructing the dislocation movement.

In the present paper an attempt is made to extend the previous investigations by the application of micro-indentation hardness testing

methods for the exploration of the early stage processes in the decomposition of the solid solution state at lower temperatures. At the same time the correlation between tensile properties and indentation hardness was studied for a series of Al-Zn-Mg alloys.

2. Experimental procedure

The investigations were carried out on a series of Al-Zn-Mg alloys. The samples were prepared from high purity, Al (99.99999%), Zn (99.9999%) and Mg (99.999%). The compositions of the alloys were determined by spectroscopic methods and are given in Table I.

Thin sheets of thickness 0.5 mm, were solution heat-treated at 480°C for 30 min and quenched in room-temperature water. The hardness testing measurements concerning the solid solution state were carried out immediately after quenching and did not take longer than 10 min.

The hardening effect of the GP zones which form during room-temperature ageing was followed throughout the natural ageing process. The effect of the completely developed zone structure was investigated by measurements carried out after 30 days of natural ageing.

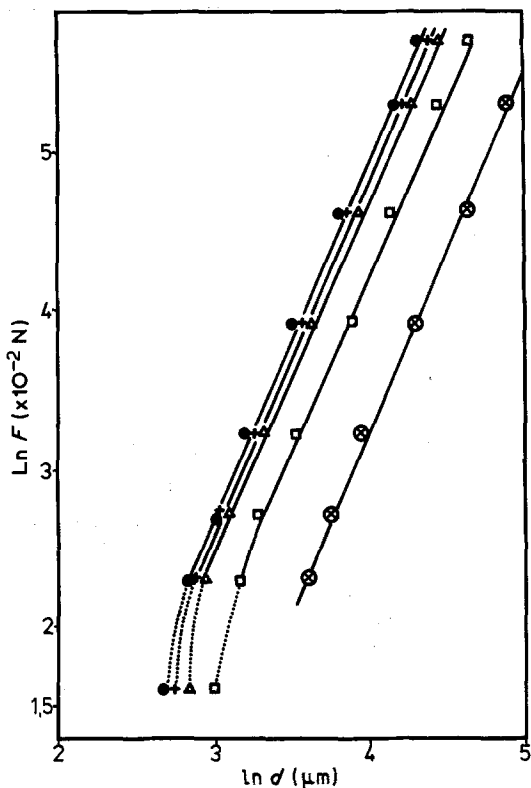


Figure 1 The load of indentation, F , against the indentation diameter, d , for high purity Al (\otimes) and Alloy 5 (Table I) after different periods of ageing at room temperature. \square As-quenched state, \triangle 3 days ageing, \circ 8 days ageing and \bullet 27 days ageing.

The microhardness measurements were made using Durimet-type Leitz microhardness testing equipment. The investigations have shown that the characteristic load dependence of microhardness disappears at large enough loads. This is shown in Fig. 1 where the applied load, F , is plotted against the indentation diameter, d , in a

double logarithmic scale for a Al (99.99999% purity) sample and for Alloy 5 (see Table I) after different ageing periods at room temperature. From Fig. 1 the microhardness, HV , values obtained with 1 N were considered to be objectively characteristic for the mechanical properties of the alloys investigated here. The rest of the HV data in the present work was therefore obtained applying a load of 1 N. Each HV value is the average of 15 to 21 indentations and has an accuracy of ± 5 to 7%.

The yield stress and the ultimate tensile strength of the samples were measured using an Instron tensile test machine at a strain rate of 2.77×10^{-3} msec $^{-1}$.

The average particle radius, R , and the volume fraction, f , of the GP zones formed at room temperature were determined by X-ray small angle scattering (XSAS). A Kratky camera with $\text{CuK}\alpha$ radiation was used in the usual way as described elsewhere [8]. From the intensity distribution curves, a Guinier plot was constructed which yielded the radius of gyration, R_g . Assuming that the GP zones formed at room temperature are spherical in shape the average particle radius, R , was obtained from the simple relation $R \cong 1.29 R_g$. By the application of a standard lupolen sample the absolute integral intensity was also obtained. In previous work the miscibility gap for room temperature was determined in a wide composition range of Al-Zn-Mg alloys [8]. On the basis of this, the volume fraction, f , of the room-temperature GP zones was calculated from the integral intensity data in the usual manner [9, 10].

3. Results and discussion

The incremental microhardness values, ΔHV , of the different Al-Zn-Mg alloys related to the microhardness of 99.99999% Al ($HV_{\text{Al}} = 238$ MPa)

TABLE I

Alloy	Composition (at %)		As-quenched state HV (MPa)	Fully zoned state				
	Zn	Mg		HV (MPa)	$\sigma_{0.02}$ (MPa)	σ_u (MPa)	f (%)	R (nm)
1	1.01	0.61	82.0	130	45	110	0.62	1.52
2	1.48	1.21	212.0	440	105	220	1.75	1.5
3	1.86	1.67	372.0	740	165	320	2.66	1.34
4	2.48	3.33	682.0	1010	255	390	4.15	1.28
5	2.00	1.5	272.0	602	-	-	1.8	1.3
6	4.00	2.5	452.0	1102	-	-	4.15	1.3
7	4.00	4.0	792.0	1340	-	-	6.5	1.55
8	4.00	1.5	140.0	662	-	-	2.75	1.35
9	1.82	1.7	-	660	161	298	2.03	1.4
10	1.45	2.75	-	620	152	290	1.21	1.3

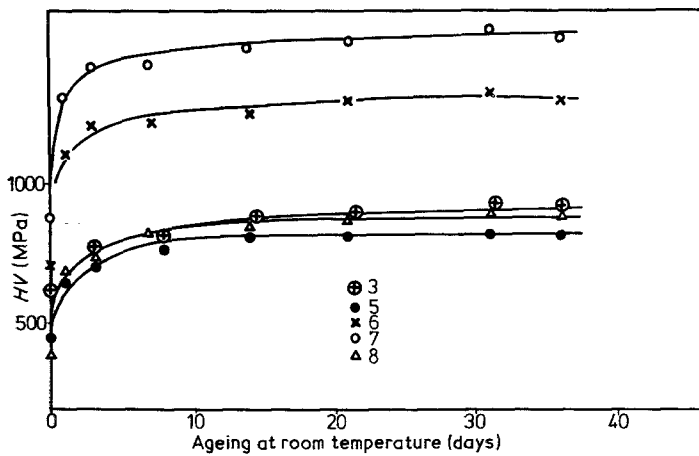


Figure 2 HV plotted against ageing time at room temperature for different alloys.

are given in Table I. The ΔHV data correspond to the solid solution state as well as to the fully zoned state obtained after 30 days natural ageing. The microhardness of the different alloys increases monotonously with the time of natural ageing after quenching. Fig. 2 shows increase in microhardness as a function of ageing time at room temperature for a few selected alloys. The behaviour of the other alloys is very similar. After a relatively fast initial increase in hardness a considerable slowing down can be observed after one week at room temperature. After 30 days the hardening can be considered to be completed. The data in Table I and the curves in Fig. 2 indicate that the hardness of the different alloys is strongly dependent on the composition after both quenching from 480°C and ageing naturally at room temperature.

Fig. 3 shows ΔHV data for alloys in which either the Zn or Mg content is constant. At fixed Zn concentration, C_{Zn} ($C_{\text{Zn}} = 4 \text{ at}\%$) the microhardness of the samples increases monotonously with increasing Mg concentration in both states, after quenching and after long-term natural ageing. At fixed Mg concentration ($C_{\text{Mg}} = 1.5 \text{ at}\%$), however, the microhardness also increases after 30 days natural ageing, but it decreases in the as-quenched state with increasing Zn content. This latter, somewhat anomalous behaviour of ΔHV may be explained as follows.

The correlation between the increment of microhardness and the composition of the alloys was investigated in the following way

$$\Delta HV = A(C_{\text{Mg}} - \alpha C_{\text{Zn}}), \quad (1)$$

where A and α are supposed to be constants and

C_{Mg} and C_{Zn} are the Mg and Zn concentration of the alloys in at%. The best approximation was obtained with $\alpha = 0.25$. Fig. 4 shows that in this case the measured ΔHV values fit a single straight line as a function of $(C_{\text{Mg}} - 0.25 C_{\text{Zn}})$ well. The value of A was found to be 264 ± 6 by the least squares method. Equation 1 with $\alpha = 0.25$ suggests that four Zn atoms compensate fully for the effect of one Mg atom in the hardness increment. This result is in full agreement with the well known fact

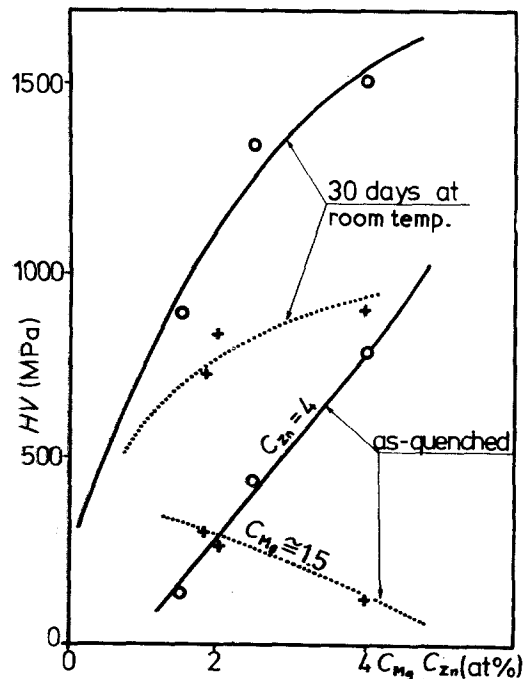


Figure 3 HV as a function of the Zn and Mg content of the alloys at fixed Mg and Zn contents in the as-quenched and in the fully zoned states.

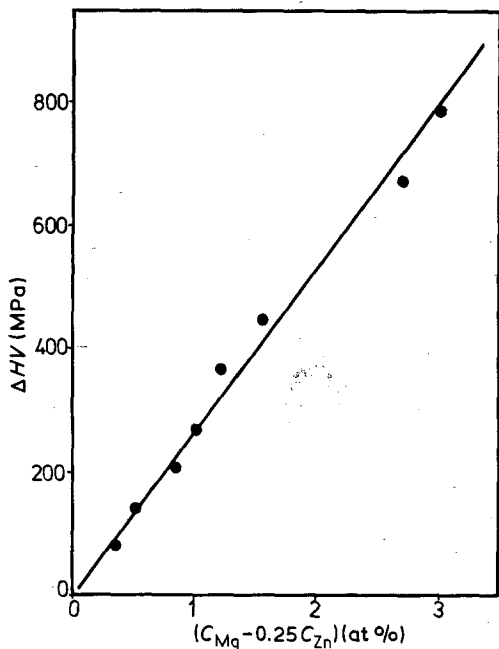


Figure 4 ΔHV as a function of $(C_{Mg} - 0.25 C_{Zn})$ at % in the as-quenched state for the different alloys.

that for Mg, $\Delta V/V = 40.8\%$ (a large positive value), whereas for Zn $\Delta V/V = 5.74\%$ (a negative size effect in the aluminium matrix) [11]. By forming small clusters around Mg the Zn atoms can reduce the lattice strains caused by the large size of the Mg atoms.

This compensating effect can only be realized, however, if the Zn atoms are situated in the vicinity of the Mg atoms. Taking this into account, it can be assumed that, even in the as-quenched solid solution state, the Mg and Zn atoms are forming small clusters before the nucleation of zone formation starts. These conclusions are strongly supported by the recent neutron scattering experiments of Auger *et al.* [12] according to which the zone formation in the same type of Al-Zn-Mg alloys is preceded by the formation of some clusters which disappear in a later stage of zone formation.

It has to be noted, however, that the value $C = C_{Mg} - 0.25 C_{Zn}$ cannot be considered as an effective Mg concentration since the hardening effect of Mg in the binary Al-Mg alloy is only 54 MPa for one atomic per cent Mg [13].

The effect of GP zones on the yield stress of Al-Zn-Mg alloys has been studied recently by Kovács *et al.* [7]. It was found that the zones are sheared by the moving dislocations during the course of plastic deformation. This mechanism can

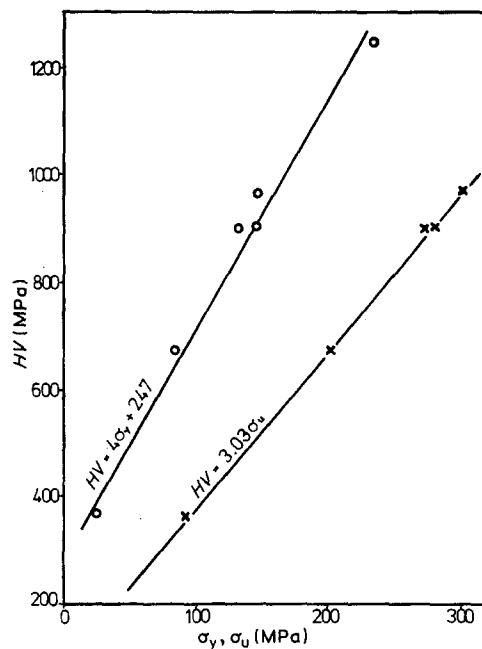


Figure 5 Correlation between HV and the yield stress, and the ultimate tensile strength, σ_u , in the fully zoned state of the alloys.

increase the yield stress strongly but has practically no effect on the rate of strain hardening. The increment of the yield stress was found to be proportional to the square root of the average zone radius, R , and to their volume fraction in the case of the same zone composition.

The correlation between the microhardness and the yield stress as well as the ultimate tensile strength, σ_u , is shown in Fig. 5 for the different alloys aged for a long time at room temperature. The figure indicates that microhardness is related linearly to both the yield stress and the ultimate tensile strength. The experimental values were fitted by the least squares method and the following relations were obtained

$$HV = 4\sigma_{0.02} + 247, \quad (2)$$

$$HV = 3.03\sigma_u. \quad (3)$$

Equation 3 is in good agreement with the generally accepted relation, $HV \cong 3\sigma_u$ [14].

On the basis of Equation 3 the correlation between ΔHV and the quantity $(fR)^{1/2}$, characteristic of the zone structure, was analysed as shown in Fig. 6. It can be seen that the microhardness of the different alloys in the fully zoned state is, to a good approximation, proportional to $(fR)^{1/2}$. This result is similar to that found for the yield

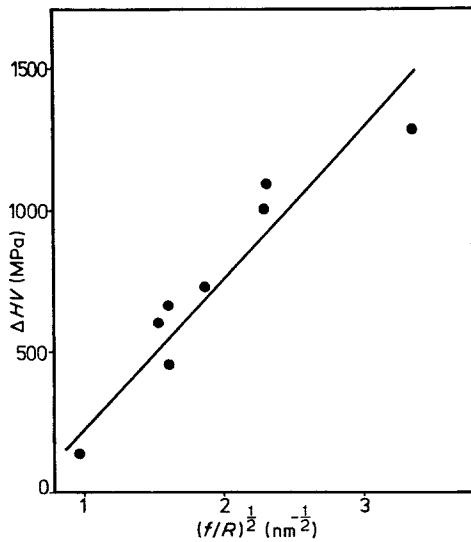


Figure 6 ΔHV as a function of $(f/R)^{1/2}$ in the fully zoned state of the different alloys.

stress in a previous work [7]. The relatively large scattering of the experimental values is most probably due to the variation in the zone composition in the different alloys [9].

The analysis of the microhardness data with respect to the average radius and the volume fraction of the GP zones, yields evidence for the shearing mechanism in the strengthening of the alloys studied here.

Since the room-temperature zones increase the yield stress of the alloys but have practically no influence on the work hardening process it can be assumed that the dislocation structure will be the same in the different alloys if the deformation caused by the indentation is the same. The same deformation, i.e. same indentation diameter in different alloys, is produced, however, by different loads. Denoting the load by F and the indentation depth by b , the work done by the indenter, W , is

$$W = F \cdot b. \quad (4)$$

The indentation diameter, d , is related to b by $b = d/7$ due to the geometry of the indenter [14].

Our experiments have shown that to produce the same indentation diameter, d_0 , larger loads were necessary for alloys compared with pure Al. The incremental load ensures the extra work necessary to cut the zones by dislocations in the alloys. Taking into account that the zones with radius R are distributed randomly in the matrix, it is easy to show that the average area of a zone lying on the slip plane of the moving dislocation is

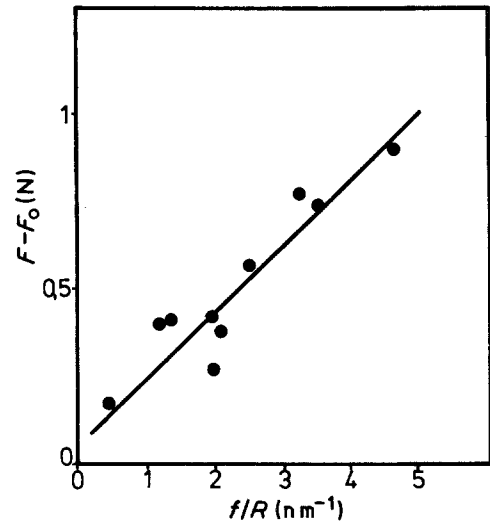


Figure 7 The extra load necessary to produce the same indentation diameter relative to that of pure Al as a function of f/R .

$2R^2\pi/3$. Obviously the number of zones cut through by a dislocation is proportional to the volume fraction of the zones. Therefore the excess work needed for cutting the zones can be written as

$$(F - F_0) \frac{d_0}{7} = \frac{2}{3} \alpha' \pi R^2 \Gamma \frac{f}{V_z} V_i, \quad (5)$$

where F and F_0 are the load values for the alloy and for pure Al, Γ is the specific surface energy necessary for shearing the zones, V_z is the average volume of a single zone, V_i is the volume of the plastic domain surrounding the indentation mark and α' is a constant taking into account the multiple shearing of the zones. Since $V_z \sim R^3$, Equation 5 can be reduced to

$$(F - F_0) \frac{d_0}{7} = A_0 \frac{f}{R} \Gamma, \quad (6)$$

where A_0 comprises all the proportionality constants.

The $(F - F_0)$ values relative to the indentation diameter, $d_0 = 35 \mu\text{m}$ are plotted as a function of f/R in Fig. 7. It can be seen that Equation 6 is fairly well satisfied. The dependence of the specific surface energy, Γ on the composition of zones [7] accounts for the scattering of the experimental values.

Acknowledgement

The authors are grateful to Aluterv-FKI, Budapest, for providing the samples.

References

1. I. J. POLMEAR, *J. Inst. Met.* **86** (1957) 24, 113.
2. H. SCHMALZRIED and V. GEROLD, *Z. Metallkde* **49** (1958) 291.
3. L. F. MONDOLFO, *Met. Rev.* **153** (1971) 95.
4. G. GROMA, E. KOVÁCS-CSETÉNYI, I. KOVÁCS, J. LENDVAI and T. UNGÁR, *Z. Metallkde* **67** (1976) 404.
5. T. UNGÁR, J. LENDVAI and I. KOVÁCS, *Aluminium* **55** (1979) 663.
6. S. C. CHANG, M. T. JAHN, C. M. WAN, J. Y. M. LEE and T. K. HUS, *J. Mater. Sci.* **11** (1976) 623.
7. I. KOVÁCS, J. LENDVAI, T. UNGÁR, G. GROMA and J. LAKNER, *Acta Met.*, in press.
8. T. UNGÁR, J. LENDVAI, I. KOVÁCS, G. GROMA and E. KOVÁCS-CSETÉNYI, *Z. Metallkde.* **67** (1976) 683.
9. G. GROMA, E. KOVÁCS-CSETÉNYI, I. KOVÁCS, J. LENDVAI and T. UNGÁR, *Phil. Mag.* **40** (1979) 653.
10. V. GEROLD in "Small Angle X-ray Scattering", edited by H. Brumberger (Gordon and Breach, New York, 1966).
11. H. W. KING, *J. Mater. Sci.* **1** (1966) 79.
12. P. AUGER, M. BERNOLE, O. BLASCHKO, G. ERNST, G. QUITTNER, W. JUST and M. ROTH, *Scripta Met.* **12** (1978) 583.
13. R. P. REED, *Cryogenics* **12** (1972) 259.
14. D. TABOR, "The Hardness of Metals" (Clarendon Press, Oxford, 1957).

Received 22 May and accepted 1 June 1980.